Particle Cosmology

Thermodynamic constraints and observational validation of the deceleration parameter

Y. Myrzakulov [a], O. Donmez [b], M. Koussour [c],*, S. Muminov [d], A. Dauletov [e], J. Rayimbaev [f,g]

[a] Department of General & Theoretical Physics, L.N. Gumilyov Eurasian National University, Astana, 010008, Kazakhstan
[b] College of Engineering and Technology, American University of the Middle East, Egaila 54200, Kuwait
[c] Department of Physics, University of Hassan II Casablanca, Morocco
[d] Mamun University, Bolkhovuz Street 2, Khiva 220900, Uzbekistan
[e] Department of Digital Technologies, Alfraganus University, Yukori Karakamish Street 2a, Tashkent 100190, Uzbekistan
[f] New Uzbekistan University, Movarounnahr Street 1, Tashkent 100007, Uzbekistan
[g] Urgench State University, Kh. Alimjan Str. 14, Urgench 221100, Uzbekistan

A R T I C L E   I N F O

A B S T R A C T

In this work, we propose a two-parameter parametrization for the deceleration parameter $q(z)$ grounded in thermodynamic constraints and applied it to explore the evolution of the universe. The second law of thermodynamics imposes essential conditions to ensure that the system approaches equilibrium in late times, requiring $q(z) \geq -1$ and $\frac{dq}{dz} > 0$ as $z \to -1$. These constraints ensure that entropy does not decrease, stabilize the system, and facilitate a smooth transition from deceleration to acceleration, consistent with the observed cosmic expansion. Furthermore, the model avoids the phantom regime ($\omega < -1$), preventing catastrophic future scenarios such as the Big Rip. Using the combined CC, Pantheon, SH0ES, and BAO datasets, we constrain the model parameters and compare the results with the standard ΛCDM model. Our findings indicate $H_0 = 70.82 \pm 0.88$, with a transition redshift of $z_t = 0.597 \pm 0.214$, suggesting an earlier onset of acceleration compared to ΛCDM. The present deceleration parameter, $q_0 = -0.364 \pm 0.032$, implies a weaker acceleration than in ΛCDM. Moreover, we analyze the evolution of total energy density, pressure, and the effective equation of state parameter, confirming a quintessence-like behavior with $\omega_0 = -0.570 \pm 0.056$. Our results provide a thermodynamically consistent framework for cosmic expansion, supporting a dark-energy-driven acceleration.

1. Introduction

Recent astronomical observations highly recommend that the universe is currently undergoing an accelerated expansion phase, a phenomenon first revealed by studies of Type Ia supernovae (SNe Ia) [1–3] and further supported by a variety of observational datasets, including large-scale structure (LSS) [4,5], Wilkinson Microwave Anisotropy Probe (WMAP) [6], cosmic microwave background (CMB) radiation [7,8], and baryon acoustic oscillations (BAO) [9,10]. The enigmatic component driving this accelerated

expansion is referred to as "dark energy" (DE), which constitutes nearly 70% of the total energy density of the universe. Despite its dominance, the exact nature of DE remains elusive and has faced significant challenges. The simplest and most widely accepted model is the standard ΛCDM model, which combines a cosmological constant (Λ) with cold dark matter [11]. Although ΛCDM successfully explains many cosmological observations, it suffers from several theoretical challenges, such as the extreme fine-tuning required to explain the small observed value of Λ and the coincidence problem, which questions why the energy densities of matter and Λ are of the same order of magnitude precisely at the current epoch [12–14]. To address these issues, alternative theories and models have been proposed, ranging from modifications of general relativity to the introduction of exotic forms of matter. Scalar field theories, both canonical and non-canonical, have emerged as prominent frameworks for describing the evolution of the universe. These include models such as quintessence [15,16], K-essence [17–19], phantom fields [20–22], tachyon fields [23,24], and Chaplygin gas [25–27]. Each of these attempts to provide a theoretical underpinning for DE and its role in cosmic evolution, offering various explanations for the transition from a decelerating to an accelerating universe.

Motivated by these issues, extensive research has been directed toward alternative approaches, including modifications of the deceleration parameter q and its relation to thermodynamic constraints [28–34]. The deceleration parameter, $q = -\frac{\ddot{a}}{aH^2}$, plays a fundamental role in characterizing the expansion history of the universe. Its significance lies in its ability to quantify the transition between the deceleration ($\ddot{a} < 0$, i.e., $q > 0$) and acceleration ($\ddot{a} > 0$, i.e., $q < 0$) phases of cosmic evolution. Here, $H = \dot{a}/a$ is the Hubble parameter, where a represents the scale factor of the universe. Observationally, q confirms that the universe is presently in an accelerating phase ($q_0 < 0$), although uncertainties in its measurements grow significantly at higher redshifts z ($z = \frac{a_0}{a} - 1$, with $a_0 = 1$). Moreover, theoretical predictions of q based on specific cosmological models remain limited due to the lack of a robust theoretical framework that consistently matches observations across all scales. This limitation highlights the need for model-independent approaches to describe q while awaiting a more comprehensive theory of quantum gravity. To address this gap, parameterized forms of $q(z)$ in terms of redshift z have been proposed, relying on empirical and practical reasoning rather than specific cosmological models. These parametrizations aim to interpolate observational data and describe cosmic evolution, particularly at intermediate redshifts. Existing forms include $q(z) = q_0 + q_1 z$ [2], $q(z) = q_0 + q_1 z (1 + z)^{-1}$ [35], $q(z) = q_0 + q_1 z(1 + z)(1 + z^2)^{-1}$ [36], $q(z) = \frac{1}{2} + q_1(1 + z)^{-2}$ [37], $q(z) = q_0 + q_1 [1 + \ln(1 + z)]^{-1}$ [38], $q(z) = \frac{1}{2} + (q_1 z + q_2)(1 + z)^{-2}$ [39], $q(z) = -1 + \frac{3}{2}(1 + z)^{q_2}(q_1 + (1 + z)^{q_2})^{-1}$ [29], $q(z) = q_0 - q_1(\frac{(1+z)^{-\alpha} - 1}{\alpha})$ [40], $q(z) = q_0 + q_1(\frac{\ln(\alpha + z)}{1 + z} - \beta)$ [41], and others that incorporate higher-order terms or asymptotic behavior. However, many of these parametrizations suffer from limitations: Some are valid only for small redshifts ($|z| \ll 1$), while others diverge as $z \to -1$, making them unsuitable for predicting the far-future behavior of the universe. Furthermore, more complex parametrizations often require three or four free parameters, introducing unnecessary complexity without providing clear physical findings [42,43].

In this paper, we propose a novel two-parameter, model-independent parametrization of $q(z)$, designed to align with observational constraints and thermodynamic principles, such as the second law of thermodynamics, which imposes specific conditions on the evolution of entropy at the apparent horizon. By ensuring $q(z) \geq -1$ and $\frac{dq}{dz} > 0$ as $z \to -1$, our model satisfies the thermodynamic requirement for the universe to approach equilibrium at late times (see Sect. 2 for the derivation of these conditions). This construction marks a significant advantage over earlier approaches, which typically fix $q(z)$ at high redshifts while leaving q_0 (the present value) as a free parameter. Although some parametrizations are also fixed $q(z)$ at $z = -1$, these are often done arbitrarily, without a foundation in fundamental physics. Our formulation, in contrast, derives these constraints from the thermodynamics of the universe, offering a physically motivated framework for understanding the cosmic expansion. This approach ensures consistency with the observations and provides a versatile tool for exploring the dynamics of the deceleration parameter across a wide range of redshifts.

The present paper is organized as follows. In Sec. 2, we present the theoretical framework for our model and discuss the thermodynamic constraints on $q(z)$. In Sec. 3, we validate our model using observational datasets, including cosmic chronometers, Pantheon+SH0ES, and BAO, and provide interpretations of the results. In Sec. 4, we analyze the evolution of the total energy density, pressure, and the effective equation of state parameter within the context of the proposed parametrization $q(z)$. Finally, in Sec. 5, we summarize and conclude our findings. Throughout the paper, we have adopted the units $8\pi G = c = 1$.

2. Theoretical framework and thermodynamic constraints on $q(z)$

In this section, we present the thermodynamic constraints on $q(z)$ in the context of GR. The Einstein field equations form the cornerstone of GR, describing the relationship between the geometry of spacetime and the distribution of matter and energy. These equations are given by [44,45]

$$R_{\mu\nu} - \frac{1}{2} g_{\mu\nu} R = \kappa T_{\mu\nu}, \tag{1}$$

where $\kappa = \frac{8\pi G}{c^4}$, $R_{\mu\nu}$ is the Ricci curvature tensor, which encodes the way the presence of mass and energy curves spacetime. The term R is the Ricci scalar, which is the trace of the Ricci tensor and provides a scalar quantity representing the overall curvature of spacetime. The symbol $g_{\mu\nu}$ is the metric tensor, which describes the geometric structure of the spacetime and determines the distances and angles in the curved spacetime. On the right-hand side, $T_{\mu\nu}$ is the energy-momentum tensor, which represents the distribution and flow of energy and momentum in spacetime.

Furthermore, we assume that the universe is described by the Friedmann-Lemaître-Robertson-Walker (FLRW) model, which characterizes a homogeneous and isotropic universe. In this model, the universe is considered to be the same at all points and in all directions, leading to the simplification of its geometry. The metric for a spatially flat universe, which assumes zero spatial curvature (i.e. $k = 0$), is given by [46,47]

$$ds^2 = dt^2 - a^2(t)[dr^2 + r^2(d\theta^2 + sin^2\theta d\phi^2)], \tag{2}$$

where $a(t)$ is the scale factor that characterizes the expansion of the universe over time. Moreover, the energy-momentum tensor for a perfect fluid, which is assumed to have no viscosity, governs the fluid's energy density and pressure. It is given by

$$T_{\mu\nu} = (p + \rho)u_\mu u_\nu - pg_{\mu\nu}, \tag{3}$$

where p is the pressure, ρ is the energy density, and u_μ is the four-velocity of the fluid. Using the Einstein field equations (1) and the metric for a spatially flat FLRW universe (2), we can derive the field equations that govern the evolution of the universe. These equations relate the Hubble parameter H, the energy density ρ, and the pressure p of the universe. The first equation, known as the Friedmann equation, is $3H^2 = \rho$, which expresses the relationship between the energy density and the Hubble parameter. The second equation, often referred to as the acceleration equation, is: $2\dot{H} + 3H^2 = -p$, which describes the evolution of the Hubble parameter in terms of the pressure of the universe.

To describe the accelerated or decelerated nature of the cosmological expansion, we introduce the deceleration parameter q, which provides a measure of the rate of change of the expansion. The deceleration parameter is defined as:

$$q = -\frac{\ddot{a}}{aH^2} = -\frac{\dot{H}}{H^2} - 1, \tag{4}$$

where $\dot{H}$ is the time derivative of the Hubble parameter. The deceleration parameter characterizes the universe's expansion: if $q > 0$, the universe is decelerating, while if $q < 0$, the universe is accelerating. This parameter is crucial for understanding the transition from a decelerating phase, dominated by matter, to an accelerating phase, associated with DE, which drives the current accelerated expansion of the universe.

Thermodynamics plays a vital role in cosmology, particularly in understanding the universe's large-scale evolution and its connection to fundamental physical laws. As well established in physics, macroscopic systems naturally evolve towards equilibrium states, as dictated by the second law of thermodynamics. This law asserts that the entropy S, of an isolated system cannot decrease, implying $dS \geq 0$, and that, in the final stages of evolution, the entropy must approach a maximum, becoming a concave function of the relevant parameters, i.e., $d^2S < 0$ [48]. For cosmological systems, this thermodynamic principle provides essential constraints on the evolution of the universe. In FLRW cosmologies, the entropy is largely governed by the entropy of the causal horizon, particularly at late times [49]. The causal horizon, which we identify with the apparent horizon, has a radius [50]

$$\tilde{r}_A = 1/\sqrt{H^2 + ka^{-2}} \tag{5}$$

where k is the spatial curvature index, and acts as a thermodynamic boundary surface. Studies have shown that the apparent horizon is the most appropriate boundary for evaluating cosmological thermodynamics [51]. Neglecting quantum corrections, the entropy of this horizon is proportional to its surface area $\mathcal{A} = 4\pi \tilde{r}_A^2$ [50], given by:

$$S_A \propto \mathcal{A} = 4\pi(H^2 + ka^{-2})^{-1}. \tag{6}$$

In the spatially flat FLRW universe ($k = 0$), this reduces to $S_A \propto H^{-2}$. From the second law, the conditions $\mathcal{A}' \geq 0$ and $\mathcal{A}'' \leq 0$ must hold throughout the evolution of the universe, ensuring the system tends towards thermodynamic equilibrium at late times [52]. Now, by differentiating Eq. (6) with respect to the scale factor a, we obtain

$$\mathcal{A}' = \frac{d\mathcal{A}}{da} = -\frac{8\pi}{H^3}\frac{dH}{da}. \tag{7}$$

Using the chain rule, $\frac{dH}{da} = \frac{dH}{dz} \cdot \frac{dz}{da}$, where $z = \frac{1}{a} - 1$ implies $\frac{dz}{da} = -\frac{1}{a^2}$. Substituting, we obtain

$$\frac{dH}{da} = -\frac{1}{a^2}\frac{dH}{dz}. \tag{8}$$

Thus

$$\mathcal{A}' = \frac{8\pi}{H^3 a^2}\frac{dH}{dz}. \tag{9}$$

Next, using the definition of the deceleration parameter in Eq. (4) and expressing it in terms of the redshift z, we have $\frac{dH}{dz} = -H \cdot (1+z)(1+q)$. Replacing $(1+z) = \frac{1}{a}$, this becomes: $\frac{dH}{dz} = -H \cdot \frac{1+q}{a}$. Substituting back, we find

$$\mathcal{A}' = \frac{8\pi}{H^3 a^2}\left(-H \cdot \frac{1+q}{a}\right) = 2\mathcal{A}\frac{1+q}{a}. \tag{10}$$

which requires $q \geq -1$ to maintain consistency with the entropy increase condition $\mathcal{A}' \geq 0$.

Differentiating $\mathcal{A}'$ with respect to a, we obtain the second derivative as

$$\mathcal{A}'' = \frac{d}{da}\left(2\mathcal{A}\frac{1+q}{a}\right),$$

$$= 2\frac{d\mathcal{A}}{da}\frac{1+q}{a} + 2\mathcal{A}\frac{d}{da}\left(\frac{1+q}{a}\right),$$

$$= 4\mathcal{A}\left(\frac{1+q}{a}\right)^2 + 2\mathcal{A}\frac{d}{da}\left(\frac{1+q}{a}\right),$$

$$\mathcal{A}'' = 2\mathcal{A}\left[2\left(\frac{1+q}{a}\right)^2 + \frac{q'}{a} - 2\frac{1+q}{a^2}\right]. \tag{11}$$

At late times ($a \to \infty$), the dominant term in square parenthesis is $\frac{q'}{a}$. For the universe to reach thermodynamic equilibrium, the deceleration parameter must approach $q \to -1$ while its derivative satisfies $dq/da < 0$ (equivalently, $dq/dz > 0$) as $z \to -1$. This behavior guarantees that the universe transitions smoothly to a de Sitter phase, maximizing the entropy of the apparent horizon.

Inspired by the thermodynamic constraints, we propose the following parameterization for the deceleration parameter:

$$q(z) = q_1 - \frac{q_1 + 1}{(1+z)^{q_2} + 1}, \tag{12}$$

where q_1 and q_2 must be positive to satisfy the thermodynamic constraints. At very high redshift ($z \gg 1$), this form approaches asymptotically $q(z) \to q_1$. By setting $q_1 = \frac{1}{2}$, the model naturally transitions to the matter-dominated universe with $q(z) \to \frac{1}{2}$, reflecting the decelerated expansion driven by gravitational clustering of matter. At the far future limit ($z \to -1$), the parametrization yields $q(z) \to -1$, corresponding to a de Sitter-like phase dominated by DE, where the universe asymptotically approaches thermal equilibrium. Thus, the first constraint $q(z = -1) = -1$ is satisfied for all values of q_1 and q_2. In addition, the second constraint (that is, $dq/dz > 0$ as $z \to -1$) is satisfied when $q_1 > -1$ and $q_2 > 0$. For the current epoch ($z = 0$), the deceleration parameter is $q(0) = q_0 = \frac{q_1 - 1}{2}$, ensuring $q(0) < 0$, consistent with observational evidence of accelerated expansion. The smooth transition between these eras, governed by the parameter q_2, reflects the thermodynamic evolution from a decelerated matter-dominated phase to an accelerated DE-dominated phase.

In addition, the transition redshift z_t marks the shift from a decelerating to an accelerating expansion in the universe. This is the point at which the acceleration of the cosmic scale factor changes sign, often associated with the transition from matter domination to DE domination. For the proposed model, the redshift transition z_t is given by

$$z_t(q = 0) = \left(\frac{1}{q_1}\right)^{\frac{1}{q_2}} - 1. \tag{13}$$

It is important to note that we do not directly constrain the parametrizations due to the limited availability of $q(z)$ data and their significant error margins. Instead, we constrain the expressions for $H(z)$ obtained by integrating these parametrizations; specifically,

$$H(z) = H_0 \exp\left(\int_0^z \frac{q(z) + 1}{1 + z}\,dz\right). \tag{14}$$

where $H_0 = H(z = 0)$ is the Hubble constant. In addition, this approach offers the advantage of significantly larger and more robust statistical reliability. It should be noted that H_0 appears in this expression as a free parameter, with its value determined by fitting it to the observational datasets.

By substituting Eq. (12) in Eq. (14), the expression for $H(z)$ is obtained as

$$H(z) = H_0 \left(\frac{(1+z)^{q_2} + 1}{2}\right)^{\frac{q_1 + 1}{q_2}}, \tag{15}$$

where H_0, q_1, and q_2 are the model parameters, which are constrained in the next section using observational data.

3. Observational validation

In this section, we describe the process of fitting the proposed parametrization of the deceleration parameter $q(z)$, to observational data. The likelihood function is expressed as $\mathcal{L} \propto \exp(-\chi^2/2)$, where the best fit is obtained by minimizing the total chi-square value, $\chi^2_{total} = \chi^2_{CC} + \chi^2_{SNe} + \chi^2_{BAO}$. By comparing the proposed parametrizations with the observational datasets, the optimal parameter values are determined through the minimization of χ^2_{total} using the Markov Chain Monte Carlo (MCMC) method [53,54]. The analysis is performed with flat priors in physically motivated ranges: $H_0 \in [50, 100]\,\text{km/s/Mpc}$, $q_1 \in [0, 10]$, and $q_2 \in [0, 10]$.

3.1. Cosmic chronometers

The Hubble dataset provides crucial information about the expansion rate of the Universe, derived from various observational techniques. Among these, *Cosmic Chronometers (CC)* stand out as one of the most reliable methods. CC are passively evolving galaxies that no longer experience significant star formation, identified through distinct spectral and color features [55–57]. Using the CC method, 31 measurements of the Hubble parameter $H(z)$ have been obtained, spanning redshifts from 0.07 to 2.41 [58]. The determination of $H(z)$ in the CC approach relies on the relation,

$$H(z) = -\frac{1}{1+z}\frac{dz}{dt}, \tag{16}$$

where $\frac{dz}{dt}$ represents the rate of redshift change derived from galaxy age differences. Specifically, Δz is the redshift difference and Δt corresponds to the age difference between two galaxy populations.

To account for uncertainties in the CC dataset, the covariance matrix C_{ij} includes contributions from multiple sources, such as statistical errors (C_{ij}^{stat}), contamination by younger stellar populations (C_{ij}^{young}), sensitivity to modeling assumptions (C_{ij}^{model}), and metallicity effects (C_{ij}^{stemet}). The total covariance matrix is expressed as

$$C_{ij} = C_{ij}^{stat} + C_{ij}^{young} + C_{ij}^{model} + C_{ij}^{stemet}. \tag{17}$$

The model-dependent component C_{ij}^{model} is further decomposed to include specific uncertainties, such as those arising from the star formation history (C_{ij}^{SFH}), the initial mass function (C_{ij}^{IMF}), the stellar library ($C_{ij}^{Ste.Lib}$), and the population synthesis model (C_{ij}^{SPS}). This is expressed as [59]

$$C_{ij}^{model} = C_{ij}^{SFH} + C_{ij}^{IMF} + C_{ij}^{Ste.Lib} + C_{ij}^{SPS}. \tag{18}$$

For the MCMC analysis, the χ^2 function is constructed to compare the observed and theoretical Hubble parameter values. It is defined as

$$\chi^2_{Hubble} = \Delta \mathbf{H} \, C^{-1} \, \Delta \mathbf{H}^T, \tag{19}$$

where $\Delta \mathbf{H}_i = \mathbf{H}_{obs.}(z_i) - \mathbf{H}_{model}(z_i)$, and C represents the covariance matrix for the dataset.

3.2. Pantheon+SH0ES

The Pantheon+SH0ES dataset comprises 1701 light curves from 1550 spectroscopically confirmed Type SNe Ia across 18 surveys, covering a redshift range of 0.001 to 2.3 [60]. This extensive compilation provides a vital resource for probing the expansion history of the Universe over a broad temporal range. SNe Ia serve as standard candles, enabling the measurement of relative distances through their distance modulus, a key quantity in cosmological analyses. Building on previous compilations such as Union [61], Union2 [62], Union2.1 [63], JLA [64], and Pantheon [65], this updated dataset incorporates additional observations and refined statistical techniques. These enhancements address critical degeneracies and uncertainties, such as those between the Hubble constant H_0 and the absolute magnitude M. The χ^2 function for Pantheon+SH0ES data is defined as

$$\chi^2_{SNe} = D^T C_{SNe}^{-1} D, \tag{20}$$

where C_{SNe} is the covariance matrix, incorporating both statistical and systematic uncertainties. The vector D is expressed as

$$D = m_{Bi} - M - \mu^{th}(z_i), \tag{21}$$

where m_{Bi} is the apparent magnitude, M is the absolute magnitude, and $\mu^{th}(z_i)$ is the theoretical distance modulus. The theoretical distance modulus is given by

$$\mu^{th}(z_i) = 5 \log_{10} \left(\frac{D_L(z_i)}{1\,\text{Mpc}} \right) + 25, \tag{22}$$

where $D_L(z)$ is the luminosity distance, defined as

$$D_L(z) = c(1+z) \int\limits_0^z \frac{dx}{H(x,\theta)}, \tag{23}$$

with θ representing the model parameters. To mitigate the degeneracy between H_0 and M, the Pantheon+SH0ES dataset introduces a redefinition of D:

$$\bar{D} = \begin{cases} m_{Bi} - M - \mu_i^{Ceph} & \text{for Cepheid hosts,} \\ m_{Bi} - M - \mu^{th}(z_i) & \text{otherwise,} \end{cases} \tag{24}$$

where μ_i^{Ceph} is the distance modulus derived from Cepheid variables. Consequently, the χ^2 function becomes: $\chi^2_{SNe} = \bar{D}^T C_{SNe}^{-1} \bar{D}$.

3.3. BAO measurements from DESI

The BAOs serve as a powerful cosmological probe by tracing the imprints of early universe sound waves in the large-scale structure of the cosmos. These oscillations originate from primordial density fluctuations in the baryon-photon plasma before recombination. Here, we constrain cosmological models using BAO measurements from galaxy, quasar [66], and Lyman-α tracer [67] observations obtained during the first year of DE Spectroscopic Instrument (DESI) data collection, as listed in Table I of Ref. [68]. The primary observables in BAO measurements are defined as dimensionless ratios. The first is

Table 1
The best-fit values of cosmological parameters for the proposed model and ΛCDM using CC+Pantheon+SH0ES+BAO datasets.

Parameter	Model	ΛCDM
H_0	70.82 ± 0.88	71.50 ± 0.89
q_1	$0.284^{+0.048}_{-0.058}$	-
q_2	$2.69^{+2.38}_{-2.94}$	-
Ω_{m0}	-	0.321 ± 0.012
r_d	137.7 ± 2.0	139.8 ± 2.1
$\mathcal{M}$	-19.302 ± 0.027	-19.308 ± 0.027
$\Omega_{\Lambda 0}$	-	0.679 ± 0.012
q_0	-0.364 ± 0.032	-0.519 ± 0.018
ω_0	-0.570 ± 0.056	-0.679 ± 0.012
z_t	0.597 ± 0.214	0.617 ± 0.029
χ^2_{min}	1805.08	1794.32

$$\frac{d_M(z)}{r_d} = \frac{D_L(z)}{r_d(1+z)}, \tag{25}$$

where $d_M(z)$ is the transverse comoving distance, and r_d represents the sound horizon at the drag epoch, which depends on the physical energy densities of matter and baryons, as well as the effective number of extra relativistic degrees of freedom. To compute r_d, we follow the approach outlined in Ref. [9]. The second observable is the Hubble distance ratio:

$$\frac{d_H(z)}{r_d} = \frac{c}{r_d H(z)}, \tag{26}$$

where $d_H(z)$ is the Hubble distance. The third observable is the ratio of the volume-averaged angular diameter distance:

$$\frac{d_V(z)}{r_d} = \frac{[z d_M^2(z) d_H(z)]^{1/3}}{r_d}, \tag{27}$$

where $d_V(z)$ represents the volume-averaged comoving distance. Further, the χ^2 function for the BAO measurements, based on the observables $X = d_M/r_d, d_H/r_d, d_V/r_d$, is given by

$$\chi^2_{BAO} = \sum_{i=1}^{N} \left[\frac{X_i^{\text{th}} - X_i^{\text{obs}}}{\sigma_{X_i}} \right]^2, \tag{28}$$

3.4. Results

The best-fit values of the cosmological parameters for the proposed model and ΛCDM, obtained using the combined CC + Pantheon + SH0ES + BAO dataset, provide essential details on the cosmic expansion history and the transition from deceleration to acceleration. These results are presented in Table 1 and illustrated in Figs. 1 and 2. Below, we offer a detailed interpretation of these findings for the combined dataset.

Figs. 1 and 2 show the corner plots of the posterior distributions for cosmological parameters, comparing the proposed model (Fig. 1) with ΛCDM (Fig. 2) using CC, Pantheon+SHOES, and BAO datasets. The proposed model yields $H_0 = 70.82 \pm 0.88$, while ΛCDM gives $H_0 = 71.50 \pm 0.89$, showing a slight shift [69,70]. These values are notably higher than the Planck 2018 result, $H_0 = 67.4 \pm 0.5$ [71,72], highlighting the tension between late- and early-time measurements of the Hubble constant. The deceleration parameters $q_1 = 0.284^{+0.048}_{-0.058}$ and $q_2 = 2.69^{+2.38}_{-2.94}$, ensure a smooth transition from deceleration to acceleration, satisfying thermodynamic constraints and supporting the late-time acceleration scenario. Specifically, q_1 determines the present value of the deceleration parameter, directly influencing the current cosmic acceleration ($q_0 = \frac{q_1 - 1}{2}$), while q_2 governs the steepness of the transition. A larger q_2 leads to a more rapid shift from deceleration to acceleration, whereas a smaller q_2 results in a more gradual transition, reflecting the influence of the underlying cosmic dynamics. In ΛCDM, the matter density is $\Omega_{m0} = 0.321 \pm 0.012$, while the proposed model does not include Ω_{m0} explicitly, suggesting a different parametrization of cosmic acceleration. The sound horizon values, $r_d = 137.7 \pm 2.0$ (model) and $r_d = 139.8 \pm 2.1$ (ΛCDM), show minor differences and are consistent with BAO measurements, validating the model's agreement with large-scale structure data. Meanwhile, the absolute magnitude in both models, $\mathcal{M} \approx -19$, aligns with SNe distance calibrations. In ΛCDM, $\Omega_{\Lambda 0} = 0.679 \pm 0.012$, supporting the standard DE paradigm. The parameter correlations indicate a mild negative relation between H_0 and r_d, a moderate correlation between q_1 and q_2, and a weak dependence of $\mathcal{M}$ on other parameters. These results confirm a smoothly evolving deceleration parameter, with $q(z)$ transitioning from a decelerated to an accelerated phase, while H_0 remains in slight tension with Planck's CMB estimate, reflecting ongoing debates in cosmology [72].

Fig. 3 compares the evolution of the deceleration parameter $q(z)$ as a function of redshift z for the proposed model (magenta) and the standard ΛCDM model (blue). The analysis is based on constraints from the CC, Pantheon+SHOES, and BAO datasets. For both
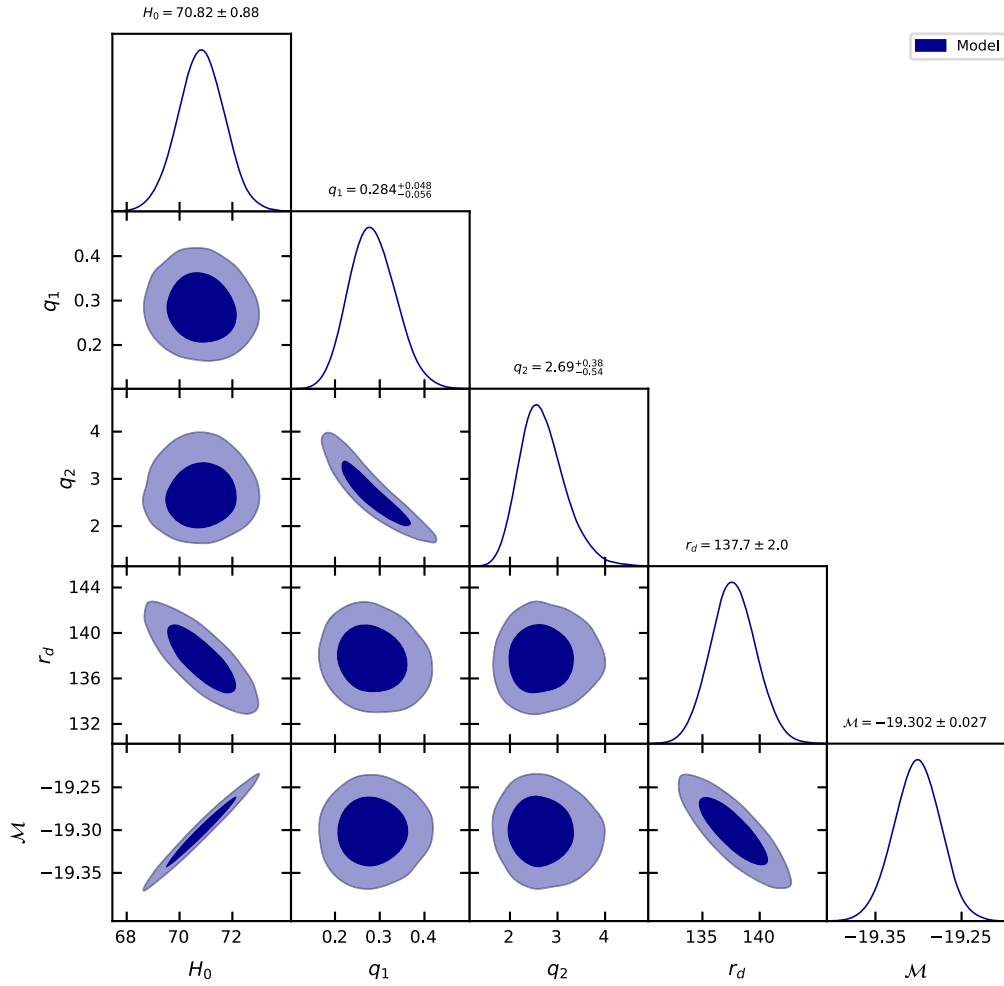
Fig. 1. The $1 - \sigma$ and $2 - \sigma$ confidence regions of cosmological parameters for the proposed model using CC+Pantheon+SH0ES+BAO datasets.

models, the universe undergoes a transition from a decelerated phase ($q > 0$) at high redshift to an accelerated phase ($q < 0$) at low redshift. The proposed model predicts a slightly earlier transition to acceleration compared to ΛCDM, indicating a modified expansion history. In the far future ($z \to -1$), both models converge to $q \approx -1$, consistent with an asymptotic de Sitter phase dominated by DE. The differences in the transition behavior and the slope of $q(z)$ highlight the impact of the additional model parameters compared to the standard cosmological paradigm.

The present values of the deceleration parameter are $q_0 = -0.364 \pm 0.032$ for the proposed model and $q_0 = -0.519 \pm 0.018$ for ΛCDM, both confirming an accelerating universe (see Table 1) [40,41,73,74]. The less negative q_0 in the proposed model suggests a weaker present-day acceleration compared to ΛCDM. Regarding the transition redshift, the proposed model gives $z_t = 0.597 \pm 0.214$, while ΛCDM yields $z_t = 0.617 \pm 0.029$, indicating a nearly similar transition epoch in both models, though the proposed model has a larger uncertainty, reflecting a broader range of possible transition times [75,76]. It is noted that the uncertainty values are obtained through standard error propagation from the posterior distributions of q_1 and q_2.

4. Evolution of energy density, pressure, and the equation of state parameter

Now, we present the evolution of key cosmological quantities—total energy density (baryonic matter+dark matter+DE), pressure, and the effective equation of state (EoS) parameter—based on the analysis of combined datasets (CC+Pantheon+SH0ES+BAO).

Fig. 4 shows the evolution of the normalized total energy density, $\rho/(3H_0^2)$, as a function of redshift z for both the proposed model (magenta) and the ΛCDM model (blue). At high redshifts ($z \gg 1$), both models predict a similar energy density evolution, indicating consistency with the standard matter-dominated era. However, at lower redshifts, subtle differences emerge, with the proposed model yielding slightly lower energy density values than ΛCDM. This deviation becomes more pronounced in the recent cosmic past and persists into the future, suggesting a modification in the underlying dynamics of cosmic acceleration. The lower energy density at low z in the proposed model implies a different rate of cosmic expansion compared to ΛCDM. This aligns with the earlier transition to acceleration observed in the deceleration parameter $q(z)$.
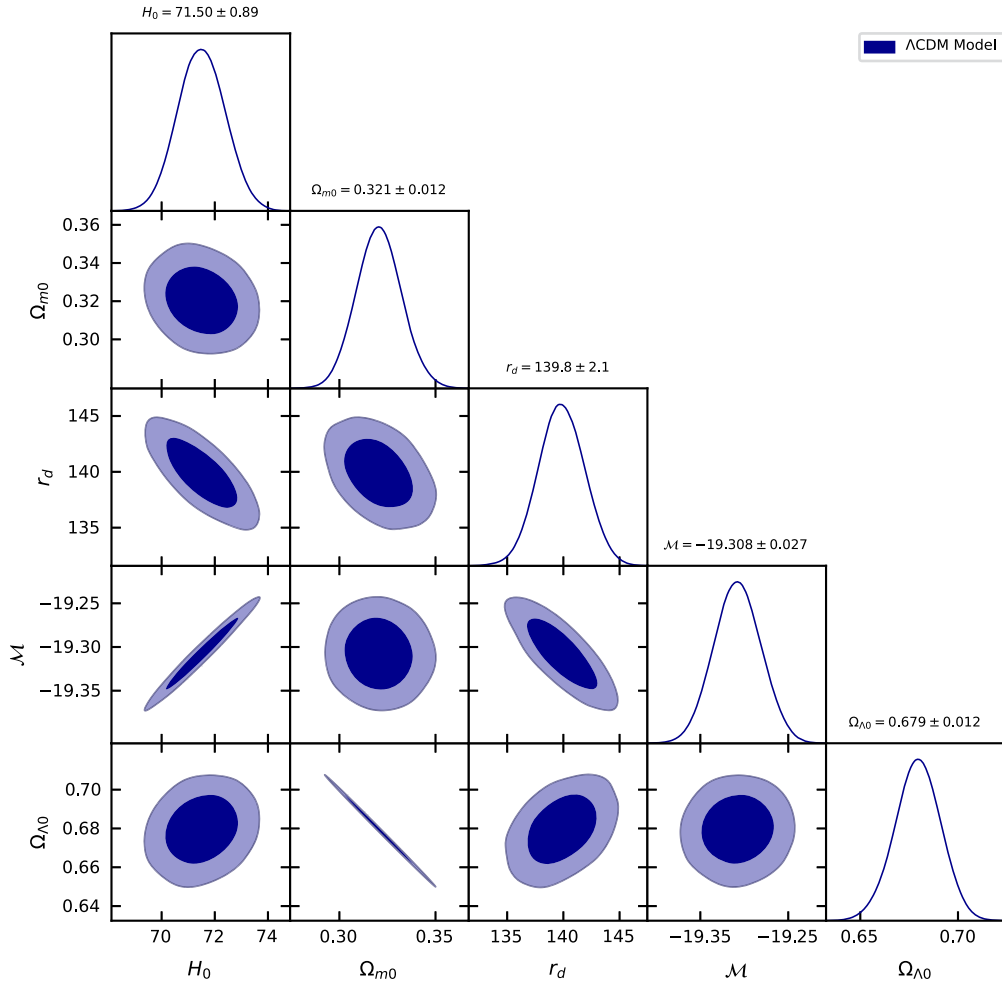
Fig. 2. The $1 - \sigma$ and $2 - \sigma$ confidence regions of cosmological parameters for the ΛCDM model using CC+Pantheon+SH0ES+BAO datasets.
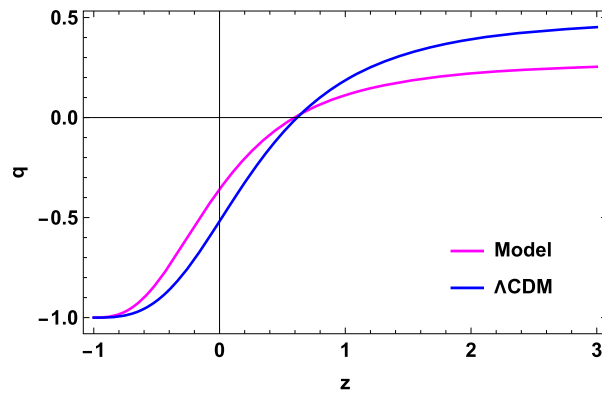

Fig. 3. The deceleration parameter q as a function of redshift z for the proposed model and ΛCDM, showing the transition from a decelerating to an accelerating universe, as constrained by observational data.

Fig. 5 illustrates the evolution of the normalized pressure, p/H_0^2, as a function of redshift z, comparing the proposed model (magenta) with the ΛCDM model (blue). In both models, the pressure is negative, but the behavior in the proposed model reflects a dynamic deviation from a cosmological constant. The negative pressure observed in the proposed model is a direct consequence of the chosen form of the deceleration parameter $q(z)$, which leads to a varying effective EoS. This evolution of pressure decreases more rapidly with redshift than in the ΛCDM model, suggesting a more significant contribution of DE at higher redshifts ($z \gg 1$) and
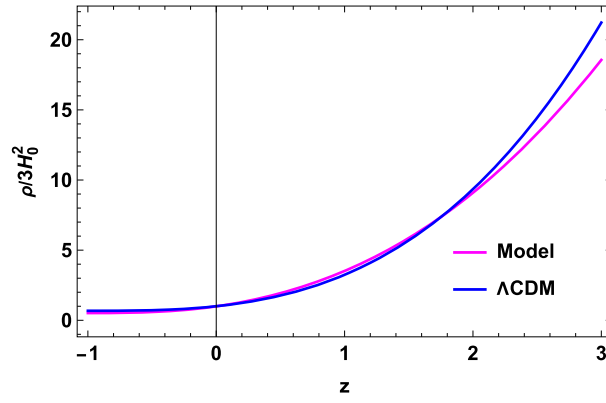
Fig. 4. The normalized total energy density $\rho/3H_0^2$, as a function of redshift z for the proposed model and ΛCDM, decreases over cosmic time.
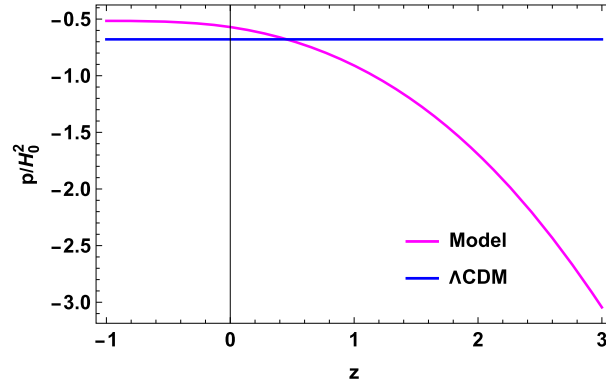

Fig. 5. The normalized total pressure, p/H_0^2, as a function of redshift z for the proposed model and ΛCDM, exhibiting negative behavior.
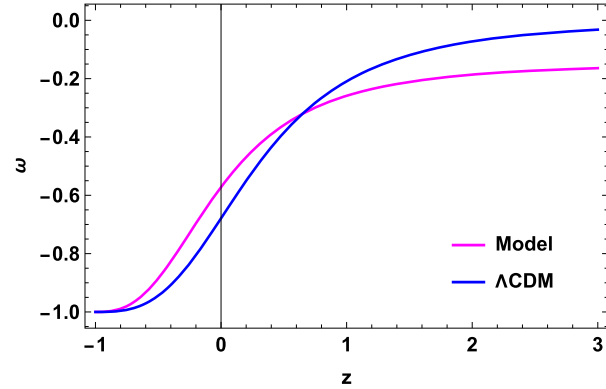

Fig. 6. The effective EoS ω as a function of redshift z for the proposed model and ΛCDM illustrates its evolution and reveals the nature of the DE component at different stages of the universe's expansion.

indicating a stronger deviation from the cosmological constant. These features reflect a modified cosmic expansion history, providing an alternative explanation for the late-time acceleration of the universe, likely driven by a dynamical DE component.

Fig. 6 highlights the evolution of the effective EoS parameter $\omega(z)$ as a function of redshift z, which is defined as the ratio of pressure to total energy density ($\omega = p/\rho$). It is important to note that this effective EoS parameter is derived from the deceleration parameter $q(z)$, rather than being assumed as a priori. This distinguishes our approach from models that directly parametrize the EoS. The figure compares the proposed model (magenta) with the standard ΛCDM model (blue). The EoS parameter categorizes the accelerating universe into three possible states: the quintessence era ($-1 < \omega < -\frac{1}{3}$), the phantom era ($\omega < -1$), and the cosmological constant era ($\omega = -1$). For both models, $\omega(z)$ transitions from a matter-dominated era ($\omega \approx 0$ at high z) to a dark-energy-dominated phase ($\omega < -\frac{1}{3}$) at low z. The value $\omega = -\frac{1}{3}$ marks the threshold between decelerated and accelerated expansion, which corresponds to a significant shift in the behavior of the universe's expansion. In Fig. 6, this transition occurs at a redshift around $z_t \approx 0.6$, highlighting

a gradual move from matter domination (with $\omega \approx 0$) to the accelerated expansion driven by DE. At $z \rightarrow -1$, both models converge to $\omega \approx -1$, indicating an asymptotic de Sitter phase. Moreover, the present value of the effective EoS parameter is $\omega_0 = -0.570 \pm 0.056$ for the proposed model and $\omega_0 = -0.679 \pm 0.012$ for ΛCDM [73,77]. The larger uncertainty in ω_0 for the proposed model reflects greater flexibility in its EoS evolution, whereas ΛCDM remains tightly constrained around a nearly constant value.

5. Conclusion

In this work, we proposed a two-parameter parametrization for the deceleration parameter $q(z)$ based on thermodynamic constraints and its application to the evolution of the universe. The thermodynamic behavior of the universe, guided by the second law of thermodynamics, imposes essential conditions for the evolution of $q(z)$. Specifically, to ensure that the system tends towards thermodynamic equilibrium at late times, we required that: $\mathcal{A}' \geq 0$ and $\mathcal{A}'' \leq 0$, where $\mathcal{A}'$ and $\mathcal{A}''$ represent the first and second derivatives of the surface area, respectively. These conditions guarantee that the entropy does not decrease and that the system reaches a stable equilibrium. From these constraints, we derived the necessary conditions for the deceleration parameter $q(z)$: $q(z) \geq -1$ and $\frac{dq}{dz} > 0$ as $z \rightarrow -1$ [48–52]. These conditions ensure that the universe remains in the quintessence era, characterized by $\omega > -1$, and avoids entering the phantom regime ($\omega < -1$), which could lead to a future catastrophic event like the Big Rip. Moreover, the second condition, $\frac{dq}{dz} > 0$, ensures that the deceleration parameter is increasing with redshift, providing a smooth transition from deceleration to acceleration, consistent with the observed cosmic expansion.

Then, we have analyzed the proposed cosmological model using the combined CC, Pantheon, SH0ES, and BAO datasets, comparing its predictions with the standard ΛCDM model. The findings shed light on the history of cosmic expansion, particularly the transition from deceleration to acceleration. The model yields $H_0 = 70.82 \pm 0.88$, slightly lower than the ΛCDM value of $H_0 = 71.50 \pm 0.89$, but both remain in tension with the Planck 2018 result. The transition redshift is $z_t = 0.597 \pm 0.214$, slightly lower than ΛCDM's $z_t = 0.617 \pm 0.029$, suggesting an earlier onset of acceleration. The present deceleration parameter, $q_0 = -0.364 \pm 0.032$, indicates weaker acceleration compared to ΛCDM (see Table 1).

In addition, we studied the evolution of the total energy density, pressure, and effective EoS parameter, confirming that the universe's expansion is consistent with a DE-dominated era. In Figs. 4 and 5, the normalized total energy density decreases as the universe expands into the far future, while the pressure becomes increasingly negative. The effective EoS parameter in Fig. 6 follows a smooth transition from the matter-dominated era to an accelerating phase, with a present value of $\omega_0 = -0.570 \pm 0.056$, suggesting a quintessence-like behavior. Our results are in agreement with previous studies, supporting the idea that the universe is currently experiencing accelerated expansion due to DE. In conclusion, our study provides a thermodynamically consistent framework for the evolution of the deceleration parameter and its application to observational data. By incorporating thermodynamic constraints, we have ensured that the model not only fits the observational data but also respects the fundamental laws governing the expansion of the universe. The findings support the universe's continuous acceleration and shed more light on the cosmological parameters that govern its evolution. Future studies incorporating additional high-precision datasets could further refine the model parameters and test its viability against the standard cosmological paradigm.

CRediT authorship contribution statement

Y. Myrzakulov: Writing – review & editing, Writing – original draft, Methodology, Investigation. **O. Donmez:** Writing – review & editing, Writing – original draft, Methodology, Investigation. **M. Koussour:** Writing – review & editing, Writing – original draft, Methodology, Investigation. **S. Muminov:** Data curation, Software, Visualization. **A. Dauletov:** Investigation, Methodology, Writing – original draft, Writing – review & editing. **J. Rayimbaev:** Writing – review & editing, Writing – original draft, Methodology, Investigation.

Declaration of competing interest

The authors declare that they have no known competing financial interests or personal relationships that could have appeared to influence the work reported in this paper.

Acknowledgements

Data availability

No data was used for the research described in the article.

References

[1] A.G. Riess, et al., Astron. J. 116 (1998) 1009.
[2] A.G. Riess, et al., Astrophys. J. 607 (2004) 665–687.

[3] S. Perlmutter, et al., Astrophys. J. 517 (1999) 377.
[4] T. Koivisto, D.F. Mota, Phys. Rev. D 73 (2006) 083502.
[5] S.F. Daniel, Phys. Rev. D 77 (2008) 103513.
[6] D.N. Spergel, et al., Astrophys. J. Suppl. 148 (2003) 175.
[7] R.R. Caldwell, M. Doran, Phys. Rev. D 69 (2004) 103517.
[8] Z.Y. Huang, et al., J. Cosmol. Astropart. Phys. 0605 (2006) 013.
[9] D.J. Eisenstein, et al., Astrophys. J. 633 (2005) 560.
[10] W.J. Percival, et al., Mon. Not. R. Astron. Soc. 401 (2010) 2148.
[11] I. Zlatev, L. Wang, P.J. Steinhardt, Phys. Rev. Lett. 82 (1999) 896.
[12] S. Weinberg, Rev. Mod. Phys. 61 (1) (1989).
[13] T. Padmanabhan, Phys. Rep. 380 (2003) 235.
[14] P.J. Steinhardt, L. Wang, I. Zlatev, Phys. Rev. D 59 (1999) 123504.
[15] B. Ratra, P.J.E. Peebles, Phys. Rev. D 37 (1998) 3406.
[16] N. Roy, Gen. Relativ. Gravit. 55 (2023) 115.
[17] T. Chiba, et al., Phys. Rev. D 62 (2000) 023511.
[18] C. Armendariz-Picon, et al., Phys. Rev. Lett. 85 (2000) 4438.
[19] S.X. Tian, Z.H. Zhu, Phys. Rev. D 103 (2021) 043518.
[20] M. Sami, A. Toporensky, Mod. Phys. Lett. A 19 (2004) 1509.
[21] M. Sami, et al., Phys. Lett. B 619 (2005) 193.
[22] E. Di Valentino, A. Mukherjee, A.A. Sen, Entropy 23 (2021) 404.
[23] T. Padmanabhan, Phys. Rev. D 66 (2002) 021301.
[24] S. Hussain, et al., Phys. Rev. D 107 (2023) 063515.
[25] M.C. Bento, et al., Phys. Rev. D 66 (2002) 043507.
[26] A.Y. Kamenshchik, et al., Phys. Lett. B 511 (2001) 265.
[27] J.M.Z. Pretel, M. Dutra, S.B. Duarte, Phys. Rev. D 109 (2024) 023524.
[28] S.K.J. Pacif, Eur. Phys. J. Plus 135 (2020) 1–34.
[29] S. Del Campo, Phys. Rev. D 86 (2012) 083509.
[30] Y. Myrzakulov, et al., Phys. Dark Universe 46 (2024) 101614.
[31] M. Koussour, et al., Phys. Dark Universe 46 (2024) 101577.
[32] K. Myrzakulov, et al., J. High Energy Astrophys. 44 (2024) 164–171.
[33] Y. Myrzakulov, et al., J. High Energy Astrophys. 43 (2024) 209–216.
[34] M. Koussour, et al., Phys. Dark Universe 45 (2024) 101527.
[35] B. Santos, J.C. Carvalho, J.S. Alcaniz, Astropart. Phys. 35 (2011) 17.
[36] A.A. Mamon, S. Das, Int. J. Mod. Phys. D 25 (2016) 1650032.
[37] R. Nair, et al., J. Cosmol. Astropart. Phys. 01 (2012) 018.
[38] L. Xu, H. Liu, Mod. Phys. Lett. A 23 (2008) 1939.
[39] Y.G. Gong, A. Wang, Phys. Rev. D 73 (2006) 083506.
[40] A.A. Mamon, Mod. Phys. Lett. A 10 (2018) 1850056.
[41] A.A. Mamon, S. Das, Eur. Phys. J. C 77 (2017) 495.
[42] R. Giostri, et al., J. Cosmol. Astropart. Phys. 03 (2012) 027.
[43] S. Arora, P.K. Sahoo, Phys. Dark Universe 45 (2024) 101510.
[44] Y. Myrzakulov, et al., J. High Energy Astrophys. 43 (2024) 209–216.
[45] Y. Myrzakulov, et al., J. High Energy Astrophys. 42 (2024) 209–216.
[46] M. Koussour, N. Myrzakulov, M.K.M. Ali, Chin. J. Phys. 91 (2024) 445–457.
[47] M. Koussour, N. Myrzakulov, M.K.M. Ali, J. High Energy Astrophys. 42 (2024) 96–103.
[48] H.B. Callen, Thermodynamics and an Introduction to Thermostatistics, John Wiley & Sons, New York, 1960.
[49] C.A. Egan, C.H. Lineweaver, Astrophys. J. 710 (2010) 1825.
[50] D. Bak, S.J. Rey, Class. Quantum Gravity 17 (2000) L83.
[51] B. Wang, Y. Gong, E. Abdalla, Phys. Rev. D 74 (2006) 083520.
[52] N. Radicella, D. Pavón, Gen. Relativ. Gravit. 44 (2012) 685.
[53] A. Lewis, S. Bridle, Phys. Rev. D 66 (2002) 103511.
[54] W.R. Gilks, S. Richardson, D.J. Spiegelhalter, Markov Chain Monte Carlo in Practice, Chapman and Hall/CRC, 1996.
[55] M. Moresco, et al., J. Cosmol. Astropart. Phys. 08 (2012) 006.
[56] M. Moresco, Mon. Not. R. Astron. Soc. 450 (2015) L16–L20.
[57] M. Moresco, J. Cosmol. Astropart. Phys. 05 (2016) 014.
[58] N. Myrzakulov, M. Koussour, D.J. Gogoi, Eur. Phys. J. C 83 (2023) 594.
[59] M. Moresco, et al., Astrophys. J. 898 (2020) 82.
[60] D.M. Scolnic, et al., Astrophys. J. 938 (2022) 113.
[61] M. Kowalski, et al., Astrophys. J. 686 (2008) 749–778.
[62] R. Amanullahet, et al., Astrophys. J. 716 (2010) 712–738.
[63] N. Suzuki, et al., Astrophys. J. 746 (2012) 85.
[64] M. Betoule, et al., Astron. Astrophys. 568 (2014) A22.
[65] D.M. Scolnic, et al., Astrophys. J. 859 (2018) 101.
[66] DESI collaboration, arXiv:2404.03000, 2024.
[67] A.G. Adame, et al., J. Cosmol. Astropart. Phys. 01 (2025) 124.
[68] A.G. Adame, et al., J. Cosmol. Astropart. Phys. 02 (2025) 021.
[69] M. Stritzinger, B. Leibundgut, Astron. Astrophys. 431 (2005) 423–431.
[70] H. Yu, B. Ratra, F.Y. Wang, Astrophys. J. 856 (2018) 3.
[71] P.A.R. Ade, et al., Astron. Astrophys. 594 (2015) A13.
[72] N. Aghanim, et al., Astron. Astrophys. 641 (2020) A6.
[73] A. Hernandez-Almada, et al., Eur. Phys. J. C 79 (2019) 12.
[74] S. Basilakos, F. Bauera, J. Sola, J. Cosmol. Astropart. Phys. 01 (2012) 050.
[75] J.F. Jesus, et al., J. Cosmol. Astropart. Phys. 053 (2020) 04.
[76] J.R. Garza, et al., Eur. Phys. J. C 79 (2019) 890.
[77] Q. Zhang, Y. Wu, J. Cosmol. Astropart. Phys. 08 (2010) 038.